Oct 17th, 12:00 AM

Experimental Research on the Behaviour of Combined Web Crippling and Bending of Steel Deck Sections

J. G. M. Kerstens

H. H. Snijder

Monique Bakker

H. Hofmeyer

Thirteenth International Specialty Conference on Cold-Formed Steel Structures
St. Louis, Missouri U.S.A., October 17-18, 1996

EXPERIMENTAL RESEARCH ON THE BEHAVIOUR OF COMBINED WEB CRIPPLING AND BENDING OF STEEL DECK SECTIONS

H. Hofmeyer[1], J.G.M. Kerstens[2], H.H. Snijder[3], M.C.M. Bakker[4]

ABSTRACT

At an interior support, sections of cold-formed steel are subjected to a concentrated load and a bending moment. Existing design rules describing the section failure at an interior support are subject to improvement and are not based on the section's physical failure behaviour. In the last decade, several analytical models have been developed that predict the section ultimate concentrated load and directly include the influence of the bending moment, so that an empirical interaction method is not needed. However, the authors believe that these models are correct only for a concentrated load and a small bending moment. In practice large bending moments occur. Therefore, the aim of the current research project is to develop an analytical model for trapezoidal hat sections subjected to a concentrated load and a bending moment as occurring in practice. The development of this model will be based on both experimental and numerical research will be carried out. In this article, a part of the experimental research will be presented.

1 INTRODUCTION

1.1 EXISTING EMPIRICAL DESIGN RULES

Sections of cold formed steel, for example trapezoidal hat sections, can fail at an interior support, due to the load actions of bending moment and concentrated load. Currently, the common used empirical method to describe the failure at an interior support is given in the interaction formula below. This method will be called the empirical interaction method.

$$\alpha\frac{M}{M_u}+\beta\frac{F}{F_u}\leq\gamma \text{ and } \frac{M}{M_u}<1 \text{ and } \frac{F}{F_u}<1$$

M and F are the actual bending moment and concentrated load acting on the section. F_u is the section's ultimate concentrated load with a negligible small bending moment acting on the section. M_u is the section's ultimate bending moment without a concentrated load acting on the section. The factors α, β, and γ are determined by fitting the curve of the empirical interaction method as good as possible to points representing the ultimate loads of sections subjected to several ratios between M/M_u and F/F_u. The curve describing the empirical interaction method is graphically shown in figure 1. In this empirical interaction method, the ultimate concentrated load F_u is predicted by the F_u curve fitting method. This method uses a empirical determined formula based on the registered ultimate loads and section parameters during three-point bending tests. These tests are carried out with small span lengths to obtain a negligible small bending moment. For the empirical interaction

1 Ph.D. student, Eindhoven Univ. of Tech. (TUE), Dep. of Struc. Design, The Netherlands
2 Professor of Structural Design, Applied Mechanics, TUE.
3 Professor of Structural Design, Steel Structures, TUE, Holland Railconsult
4 Assistent Professor, Computational Mechanics, Steel Structures, TUE

method, the ultimate bending moment M_u is predicted by using the effective width method. The F_u-curve fitting method and the effective width method are explained in [Hofm96a].

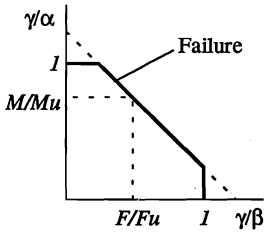

Figure 1, M/M_u-F/F_u diagram

The empirical interaction method is subject to improvement because:

- It was shown by Bakker, that the ultimate loads predicted by several F_u-curve fitting methods can differ up to 40 %. This means that the F_u-curve fitting method does not always produce accurate results [Bakk86a].

- The F_u-curve fitting method is based on three point bending tests with small span lengths. It is assumed that the bending moment is negligible small. However, this negligible small bending moment is present. For the empirical interaction method, the influence of the bending moment is thus taken into account twice: first by the interaction method itself, second by the F_u-curve fitting method.

- For some sections, the F_u-curve fitting method can not be used. Due to the section properties, the bending moment is too large to be negligible small, even for tests with very short span lengths.

- Both the empirical interaction method and F_u-curve fitting method are based on the measurement of ultimate loads during experimental tests. Both methods are not based on the section's physical failure behaviour.

1.2 FAILURE MECHANISMS

To introduce the analytical models that were developed to describe the behaviour at an interior support and will be discussed in 1.3, the section failure mechanisms for several loading conditions will be described in this paragraph.

1.2.1 CONCENTRATED LOAD AND SMALL BENDING MOMENT (F_U)

For trapezoidal hat sections, subjected to a concentrated load and a small bending moment, two failure mechanisms occur [Bakk92a]: a yield-arc mechanism and a rolling mechanism. For small corner radii, the yield-arc mechanism occurs; for large corner radii, the rolling mechanism occurs. Looking at a section's cross-section, the two failure mechanisms are shown in figure 2.

The sections are subjected to a concentrated load by a load bearing plate. The yield arc mechanism has fixed yield lines which do not move during the deformation. The rolling mechanism has moving yield lines (illustrated with an arrow). These yield lines are located at the corner radii sides. The bottom flange yield lines move under the load bearing plate to the outside direction. The web moving yield lines move up through the web to the top side. The corner radii roll in the direction of the top flange. The web crippling deformation is defined as the decrease in distance between load bearing plate and top flange, as shown in figure 2. The flange deformation has to be compatible with the web deformation. Therefore, looking at the section's side, a hinge mechanism occurs, as shown in figure 3. This hinge mechanism is equal for both mechanisms as shown in figure 2.

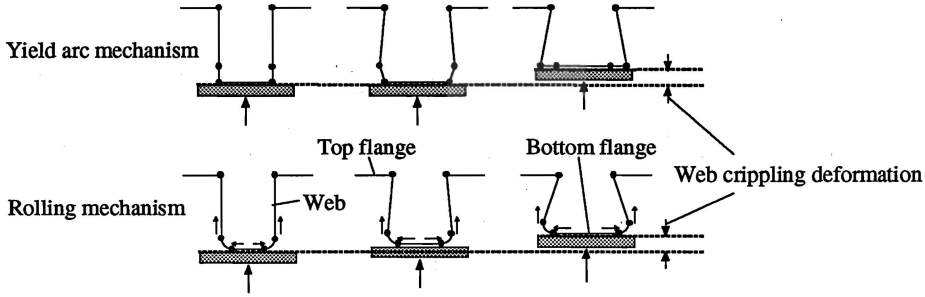

Figure 2, yield arc mechanism and rolling mechanism

Because the hinge mechanism acts like a hinge near the load bearing plate, redistribution of bending moments may be possible. This will be explained below.

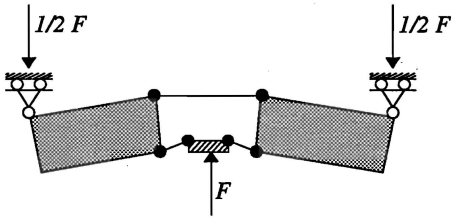

Figure 3, hinge mechanism compatible with yield arc and rolling mechanisms

In figure 4, a multi-span section is shown. If the load q for this section increases, the difference between the moment at interior support B and the moment in the field remains equal: $1/8*q*L^2$.

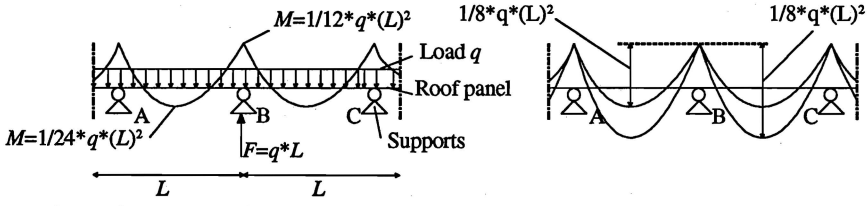

Figure 4, redistribution of bending moments

However, if the ultimate moment at B is reached because a plastic hinge has developed, the moment at B can not further increase. Therefore, the moment in the field will increase as shown in figure 4, at the right.

The section fails if the ultimate bending moment is reached both in the field and at the support. This approach is economical compared with the assumption that the section fails if either at the supports or in the field the ultimate moment is reached. However, the method of moment redistribution can only be used if there is enough rotational capacity at the support. Therefore, the hinge mechanism should have enough rotational capacity to make moment redistribution possible.

1.2.2 PURE BENDING MOMENT (M_u)

Hat sections subjected to pure bending moment only, show a failure mechanism as shown in figure 5, which is treated in literature [Dann90a, Land94a, Nest80a]. This failure mechanism will be called a bending mechanism and can have two forms. The two forms are shown in figure 5. In literature, no description was found about the web deformation mechanism (yield arc or rolling).

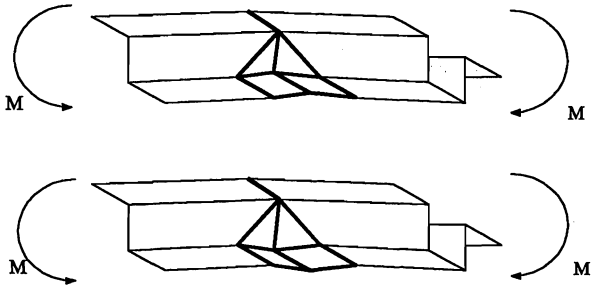

Figure 5, failure mechanisms for sections subjected to a bending moment only

1.2.3 INTERACTION (F_u AND M_u)

For sections subjected to a concentrated and a medium to large bending moment, the author did not found failure mechanisms described in literature.

1.3 EXISTING ANALYTICAL MODELS

1.3.1 FIRST GENERATION ANALYTICAL MODELS

To replace the empirical interaction method, several attempts have been carried out to develop analytical models. The developed models predict the ultimate concentrated load and directly include the influence of the bending moment, so that an empirical interaction method is not needed. They are based on the implicit assumption that the failure mechanism is not influenced by the magnitude of the bending moment. An analytical model based on this assumption will be called a first generation analytical model.

The Dutch design code for cold-formed sections incorporated a first generation analytical model in 1974. However, the correctness of this model was questionable. Reinsch presented a first

generation analytical model in 1983 [Rein83a]. For this analytical model, a yield line model of the physical failure behaviour was developed with empirically determined yield-line positions, observed in tests. Tsai calculated the section ultimate concentrated load with the Reinsch formulae and reduced this ultimate load for a small bending moment action by manipulating load-web crippling deformation curves [Tsai86a]. More information is given in [Hofm96a].

1.3.2 THE BAKKER MODEL

In 1992, Bakker presented an analytical model [Bakk92a]. The Bakker model is presented here more detailed than the first generation models because during the development of the Bakker model:

- Three different failure mechanisms were observed. Two of these mechanisms are also found in the current experimental research.
- Parameters that significantly influence the type of failure mechanism were identified. These parameters are important for the design of the current experimental research.
- Although the Bakker model was only developed for small bending moments, it was explicitly realized that the failure mechanism is influenced by the magnitude of the bending moment. Therefore the Bakker model is no first generation model.

Bakker carried out tests on trapezoidal hat sections subjected to a concentrated load only or to a concentrated load and a small bending moment. During the tests, the occurring failure mechanisms were carefully studied and the web crippling deformation, the support rotation, and the beam deflection were measured.

Three failure mechanisms were found. Two mechanisms occurred frequently: the yield-arc mechanism and the rolling mechanism. The third mechanism was characterized by an asymmetric failure and was found only 3 times. It was believed that this failure mechanism was caused by a not fully fixed load bearing plate, able to rotate slightly. More information about this mechanism is presented later.

The two failure mechanisms (rolling mechanism and yield arc mechanism) can be characterized by their concentrated load-web crippling deformation behaviour, as shown in figure 6 with bold drawn lines.

According to the Bakker model, this behaviour can be described by a linear curve until the formation of a yield line mechanism is initiated. Once this mechanism is formed, the behaviour can be described by a rigid-plastic curve, as shown in figure 6.

The mechanism initiation load is defined as the load at which the yield line mechanism is initiated. For the yield arc mechanism, the ultimate load is about the mechanism initiation load. For the rolling mechanism, the ultimate load is significantly higher than the mechanism initiation load. However, it is believed that for larger span lengths, for the rolling mechanism, the difference between mechanism initiation load and ultimate load will decrease [Bakk92a].

For the rolling mechanism, Bakker developed a yield line mechanism to predict the load F for

initiating the mechanism. For this prediction, the load F displacement w as shown in figure 7 was one of the variables used. The load F displacement w depends on the web crippling deformation and on the beam deflection as shown in figure 7. For a larger span length, both the bending moment and beam deflection increase. Because the prediction of the ultimate web crippling load F_u uses the beam deflection, the influence of the bending moment on F_u is directly taken into account.

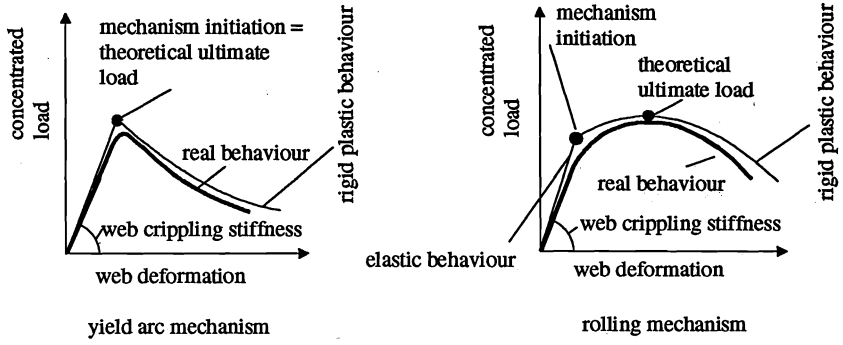

Figure 6, load deformation diagram for the yield arc and rolling mechanism

For various magnitudes of elastic web crippling deformation, Bakker calculated the load for which a yield line mechanism describing the rolling mechanism would initiate, giving a mechanism initiation curve.

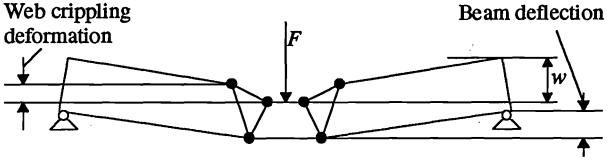

Figure 7, load displacement w equals the sum of beam deflection and web crippling deformation

For finding the linear elastic curve, Vaessen developed an analytical model [Vaes95a]. This curve is shown in figure 8. The intersection of the linear curve and mechanism initiation curve is the mechanism initiation point

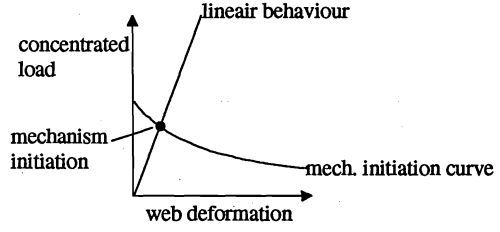

Figure 8, calculation of mechanism initiation point for the rolling mechanism

It should be noted that the mechanism initiation curve does not describe the rigid plastic behaviour and has no physical meaning, except at the mechanism initiation point.

The use of an elastic curve and a mechanism initiation curve is needed because the developed yield line mechanism for the rolling mechanism is geometrically non-linear. For geometrically linear yield line models, the mechanism initiation load can be calculated without taking elastic behaviour into account.

1.4 AIM OF CURRENT RESEARCH

First generation analytical models cannot replace the empirical interaction method because the type of failure mechanism is influenced by the magnitude of the bending moment.

This was realized by Bakker, although the Bakker model was only developed for small bending moments. In practice, medium to large bending moments occur.

The aim of the current research is to develop a new analytical model for a concentrated load and a bending moment as occurring in practice. Furthermore, the new model has to take into account that the type of failure mechanism is influenced by the magnitude of the bending moment This new model will be called a second generation analytical model. As far as known by the author, no efforts have been made so far to develop such a model.

For the development of a second generation analytical model, the failure behaviour of sections subjected to a ratio between concentrated load and bending moment as occurring in practice should be observed. These observations will be carried out first by experimental research. A part of the experimental research is presented in chapter 2.

The experimental research will be simulated using advanced finite element calculations for improving the insight about the section behaviour. Using the experimental and numerical research, a second generation analytical model will be developed.

2 EXPERIMENTAL RESEARCH

2.1 TEST SERIES DESIGN

The objective of the experimental research is to observe mechanisms of trapezoidal hat sections at an interior support, subjected to a concentrated load and a bending moment as occurring in practice.

Sections in practice have stiffeners in longitudinal and transverse direction. In this research project, first sections without stiffeners in both directions are studied. Later, sections with stiffeners in longitudinal and transverse directions will be tested.

For the experimental research, the following parameters should be equal to the situation in practice: the section properties; the ratio between the concentrated load F and the bending moment M; and the ratio between M/M_u and F/F_u. Therefore, products of two cold-formed steel manufactures were studied [Sab95a, Hair95a], the ratio between concentrated load F and bending moment M in practice was studied. Using this information, the ratio between M/M_u and F/F_u in practice could be determined. From now on, η will be defined as the ratio between M/M_u and F/F_u:

$$\eta = \frac{\left(\frac{M}{M_u}\right)}{\left(\frac{F}{F_u}\right)}$$

2.1.1 SECTION PARAMETERS

Regarding figure 9, the following test specimen parameters as occurring in practice were studied: b_{tf}, b_w, b_{bf}, θ_w, $r_{i;tf}$, $r_{i;bf}$, and t. [Hofm96c]. Furthermore, the following material properties were studied: the yield strength f_y, the ultimate strength f_u, the modulus of elasticity E, and the tensile strain at fracture ε_u.

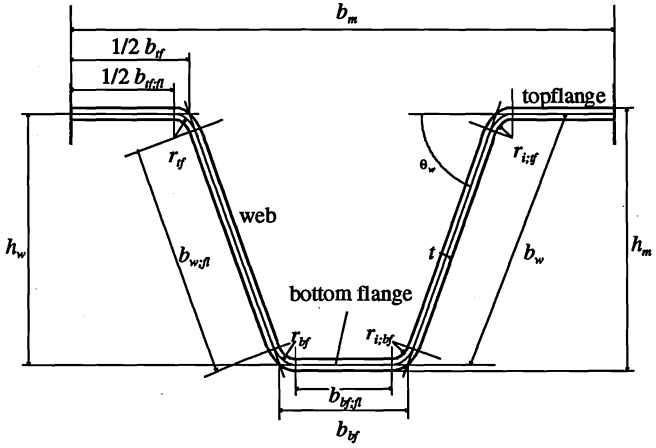

Figure 9, hat section cross-section properties

2.1.2 *M/F*-RATIOS

It was observed that in practice the *M/F* ratios equal [Hofm96c]:

$$0.55 \text{ ft } (0.167 \text{ m}) \leq \frac{M}{F} \leq 1.97 \text{ ft } (0.6 \text{ m})$$

2.1.3 η RATIOS

The η ratios occurring in practice, can be determined by calculating the ultimate bending moment M_u and the ultimate concentrated load F_u for the sections studied [Sab95a, Hair95a].

F_u is calculated using a formula developed by Wing [Wing81a] as shown below:

$$F_u = 2^{*} * 1.85^{**} * 9.0 * t^2 * f_{ty} * \sin\theta_w * \left(1.0 - 0.001 * \frac{b_w}{t}\right) * \left(1.0 + 0.005 \frac{L_{lb}}{t}\right)$$

$$* \left(1.0 - 0.075 \sqrt{\frac{r_{i;tf}}{t}}\right) * \left(1.0 - 0.1 f_{ty}\right) * \left(1.0 - 0.1 * \frac{f_{ty}}{228}\right)$$

* The ultimate load is determined for one web. In this case the ultimate load for two webs is needed.

** This factor undoes the design rule safety factor 1.85.

For the calculation of M_u, Eurocode 3 [Euro90a] and the Dutch design code RGSP'85 [Rgsp85a] are used in combination with a computer program developed by Bakker [Bakk92a]. More information is given in [Hofm96c].

The most roof panels used in practice have an η ratio between 1.45 and 2.75 as shown in figure 10.

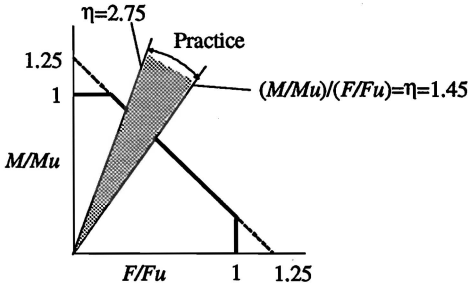

Figure 10, η ratios as occurring in practice

2.1.4 TEST SERIES

Based on the section properties, the *M/F* ratios, and the η ratios as occurring in practice, the following test series was designed. For each of the parameters, the values used in the test series are listed below:

b_{tf}:	3.94 in. (100 mm)
b_w:	3.94 in. (100 mm)
b_{bf}:	5.51 in. (140 mm)
θ_w:	50, 70, and 90 degrees
$r_{i;tf} = r_{i;bf}$:	0.0394 in., 0.118 in., 0.197 in., and 0.394 in. (1, 3, 5, and 10 mm)
t:	0.0295 in. (0.75 mm)
L:	47.2 in., 70.9 in., and 94.5 in. (200, 1800, and 2400 mm)
f_y:	46,376.8 psi (320 N/mm^2)
f_u:	56,521.7 psi (390 N/mm^2)
E:	3.04*10^7 psi (210,000 N/mm^2)
ε_u:	17 %

The values of θ_w, $r_{i;tf}$, $r_{i;bf}$, and L are variable, but $r_{i;tf}$ and $r_{i;bf}$ are equal. It was shown in the research of Bakker [Bakk92a] that the four parameters have significant influence on the type of failure. The values of b_{tf}, b_w, b_{bf}, t, f_y, f_u, E, and ε_u are constant for all test specimens, because it is assumed that these parameters have less significant influence on the type of failure [Bakk92a]. All values have been chosen to meet the values in practice. However, L and b_w were slightly adjusted until the M/F and η ratios of the test specimens equaled the situation in practice. For every combination of parameter values, a test specimen has been designed, giving 36 test specimens.

2.2 PILOT TEST SERIES

Before testing the test series discussed in 2.1.4, a pilot test series has been designed for three reasons. First, the tests series was used to develop the test setup. Furthermore, the pilot test series was set up to investigate the influence of a 'bending and rebending' zone in the bottom flange. For sections having a large ratio between section height and bottom flange width, this 'bending and rebending' zone is needed if the press brake operation is used for producing the sections. The zone is produced by bending and rebending the bottom flange in the midzone at the same position for 90 degrees, as shown in figure 11. More information is presented in [Hofm96c].

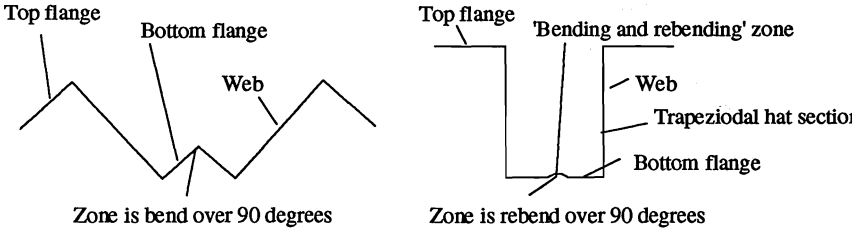

Figure 11, 'bending and rebending' zone inevitably for press-brake operation

Finally, the pilot series were used to explore the section mechanisms. Therefore θ_w, b_{bf}, and L were varied. Sections were provided with and without a 'bending en rebending' zone to investigate the influence of this zone on the failure behaviour. The pilot series is presented in the table 1.

All other section properties were constant. They were designed to be equal to:

b_{tf}:	5.51 in. (140 mm)
b_w:	3.94 in. (100 mm)
$r_{i;tf} = r_{i;bf}$:	0.118 in. (3 mm)
t:	0.0295 in. (75 mm)
f_y:	47,536.2 psi (328 N/mm^2)
f_u:	58,115.9 psi (401 N/mm^2)
E:	3.04*10^7 psi (210,000 N/mm^2)
ε_u:	33.5 %

Section*	θ_w [deg]	b_{bf} [in.]	'bending and rebending' zone	L [in.]
1	50	3.94	yes	39.4
2	70	3.94	no	39.4
3	70	3.94	yes	39.4
4	90	3.94	no	39.4
5	90	3.94	yes	39.4
6	70	1.57	yes	47.2
7	50	1.57	no	55.1
8	90	1.57	yes	55.1
9	50	1.57	no	63.0
10	90	1.57	no	63.0
11	70	1.57	yes	70.9
12	90	1.57	yes	70.9
13	90	1.57	yes	70.9

* section numbers are specified in report [Hofm96c]

Table 1, pilot test series

2.3 TEST SETUP

In the tests, the sections of the pilot test series were subjected to a concentrated load and a medium to large bending moment, as shown in figure 12.

The sections were loaded by a load bearing plate, fastened to a hydraulic jack. The hat sections were supported by support rods and bars at the section ends. Strips, preventing spreading of the webs, were fixed on the section upper flanges. Two strips preventing sway of the section webs and bottom flange were fixed on the section ends.

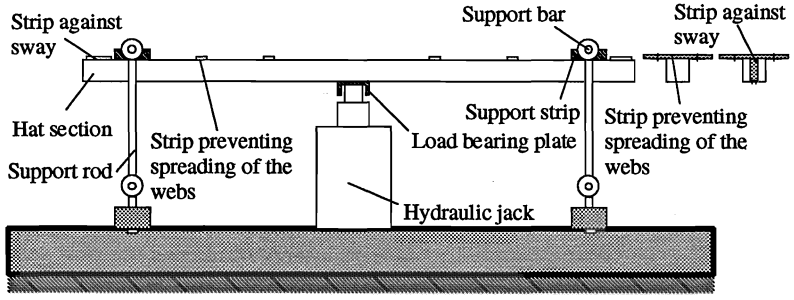

Figure 12, test rig, mechanical part

Measurements were carried out as shown in figure 13. The support rotations were measured using two displacement indicators measuring the displacement of a frame fixed to the support rods. The support rotations are registered to investigate the bending moment-rotation behaviour used for moment redistribution as explained in 1.3. The web crippling deformation was measured using two Linear Variable Differential Transformers (LVDT) fastened at a measurement strip. This strip was fixed at the upper flanges. The LVDT units measured the displacement between this strip and the load bearing plate. The web crippling deformation was measured to investigate the relation

between web crippling deformation and concentrated load and to investigate the relation between web crippling deformation and support rotation.

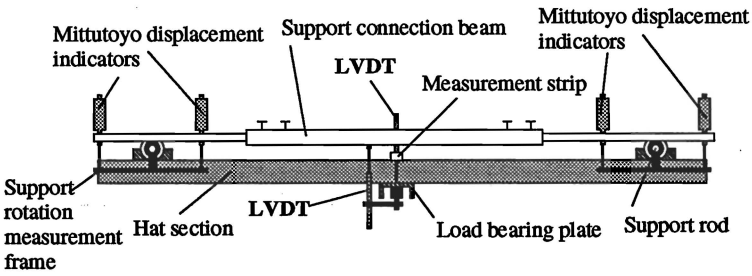

Figure 13, test rig, measurement part

The beam deflection was measured using one LVDT measuring the distance between the load bearing plate and the support connection beam.

2.4 TEST RESULTS

2.4.1 OCCURRING FAILURE MODES AND MECHANISMS

To describe the section failure behaviour, distinction has been made between the section behaviour at ultimate load and the section post-collapse behaviour. Failure modes will describe the behaviour at ultimate load and failure mechanisms will describe the post-collapse behaviour. During the pilot tests two failure modes were observed, as shown in figure 14.

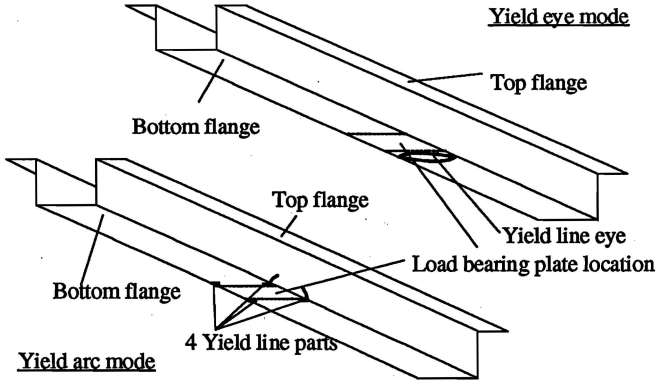

Figure 14, section behaviour at ultimate load

For one failure mode, the webs were locally indented at the four corners of the load bearing plate, seeming to form a yield arc in the webs. This mode will be called the yield arc mode. For the other

failure mode, two curved yield lines, that have the appearance of an eye, occurred in the bottom flange besides the load bearing plate. This mode will be called the yield eye mode.

It is believed that the yield eye mode is caused by bending moment mainly and that the yield arc mode is caused by the concentrated load mainly.

For the yield eye mode, at ultimate load, the tests showed that the bottom flange fails first, due to compression stresses in longitudinal direction. Compression stresses in the bottom flange in longitudinal direction are mainly introduced by the bending moment.

For the yield arc mode, at ultimate load, the tests showed that the webs fail first, due to compressive stresses in the web. Compressive stresses in the webs in transversal direction are mainly introduced by the concentrated load.

After the attainment of the ultimate load, three mechanisms occurred as shown in figure 15: the yield arc mechanism, the yield eye mechanism and the interaction mechanism.

The yield arc mechanism developed from the yield arc mode. The flange deformed to be compatible with the deforming webs of the yield arc mode. The yield eye mechanism developed from the yield eye mode. The webs deformed to be compatible with the deforming flange of the yield eye mode. The interaction mechanism developed from the yield arc mechanism after large deformations.

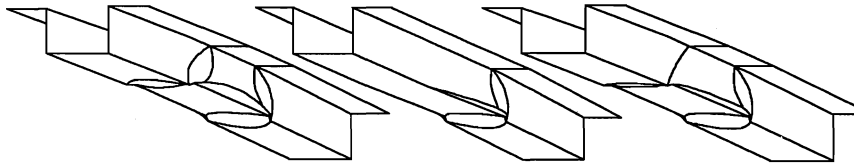

Yield arc mechanism Yield eye mechanism Interaction mechanism

Figure 15, yield line mechanisms for post-collapse behaviour

For all mechanisms, the top flange yield lines were not clearly marked during the tests. However, they are shown in figure 15 to indicate the hinge mechanism develops.

2.4.3 LOAD-WEB CRIPPLING DEFORMATION AND BENDING MOMENT-ROTATION BEHAVIOUR

For all test specimens, the load-web crippling deformation behaviour of the yield arc, the yield eye and the interaction mechanism is given in figure 16. For all mechanisms, the load decreases fast after the ultimate load. The web crippling deformation for the yield eye mechanism seems to decrease after the ultimate load. However, this is not true, but is caused by lifting of the test specimen from the load bearing plate, giving a wrong indication for the web crippling deformation as shown in figure 18. The lifting of the test specimen is characteristic for the yield eye mechanism. The interaction mechanism acts first as a yield arc mechanism, thereafter, the behaviour of the yield eye mechanism is followed.

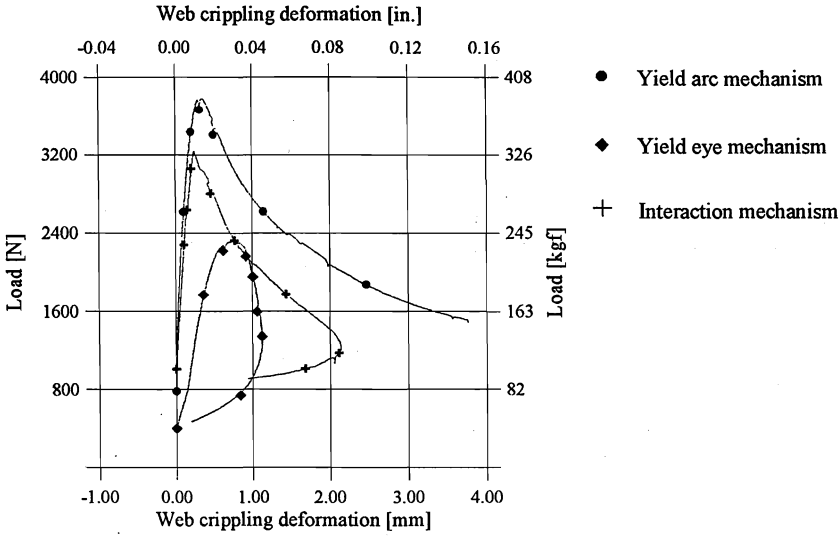

Figure 16, load-web crippling deformation for three mechanisms

For all test specimens, for all failure mechanisms, the same bending moment-support rotation behaviour occurred. This behaviour is shown in figure 17.

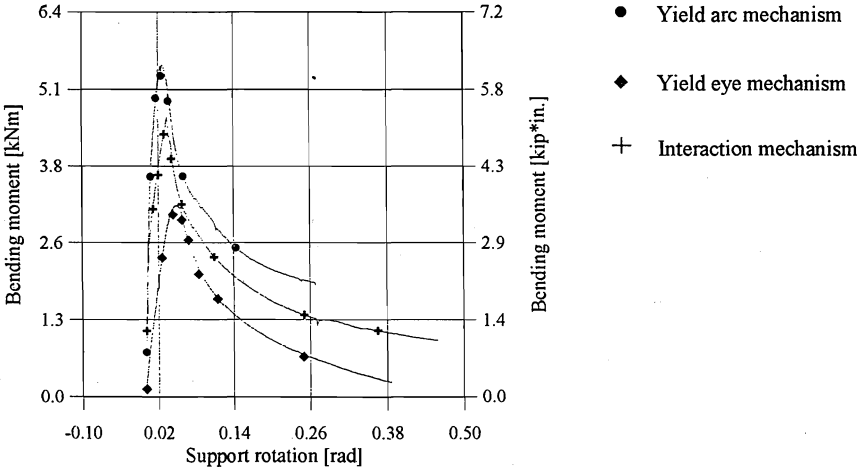

Figure 17, bending moment-support rotation behaviour for three mechanisms

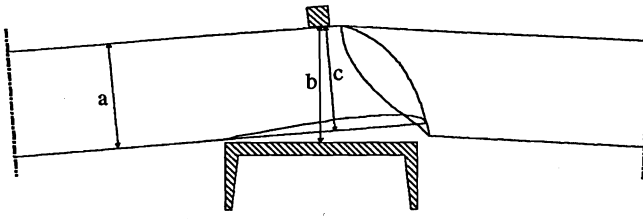

a = real section height
a-c = real web crippling deformation
a-b = measured web crippling deformation

Figure 18, measured web crippling deformation

2.4.4 LOCATION OF TEST RESULTS IN F/F_u AND M/M_u DIAGRAM

The test specimens F/F_u and M/M_u values are presented in figure 19. F_u and M_u were calculated as mentioned in 2.1.3. The sections with a 'bending and rebending' zone have probably a higher M_u. This was not taken into account, because no design rules were available to calculate the increased M_u caused by the 'bending and rebending' zone. F and M were registered during the tests.

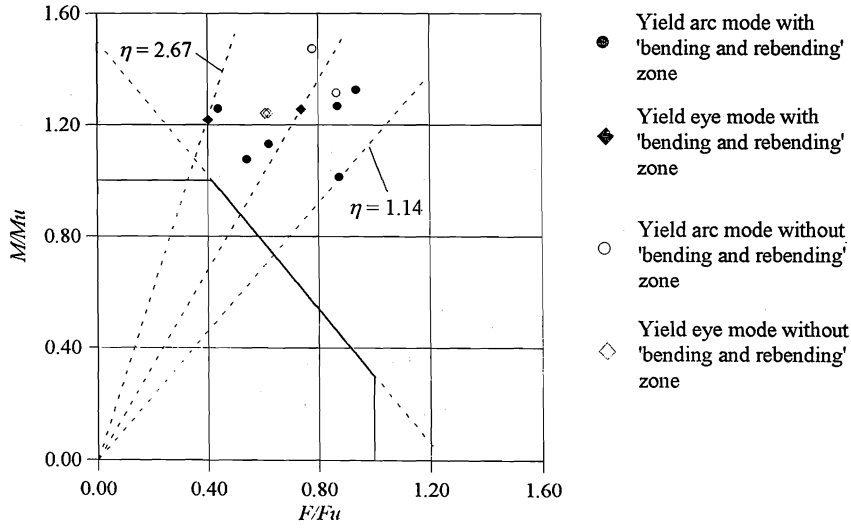

Figure 19, M/M_u and F/F_u values for tested hat sections

The sections failed by the yield eye mechanism are located in the group with the highest η ratios (figure 19). The sections failed by the yield eye mechanism are located on an almost horizontal

line. This indicates that for these sections, the ultimate load depends not on the F/F_u ratio. However, this indication is only based on 3 tests.

In figure 19, it can also be seen that the test series has η ratios between 1.14 and 2.67. Following paragraph 2.2 the η ratios should lie between 1.45 and 2.75. This means that for the η ratio the test series represent the situation in practice.

3 DISCUSSION ABOUT OBSERVATIONS DURING EXPERIMENTAL TESTS

3.1 'BENDING AND REBENDING' ZONE

During the tests, no significant influence of the 'bending and rebending' zone on the failure mechanism type was found. However, sections having the 'bending and rebending zone' had a 10 % higher ultimate load compared with sections not having the 'bending and rebending' zone. It is believed that this is caused by the higher yield strength of the 'bending and rebending zone', due to the fabrication process.

3.2 FAILURE MODES: YIELD ARC MODE AND YIELD EYE MODE

For trapezoidal hat sections, having small corner radii, at the ultimate load two failure modes were found: the yield arc mode and the yield eye mode.

For small η ratios, without exception, the yield arc mode occurred. This was also found by Bakker [Bakk92a]. For large η ratios, the yield arc mode and the yield eye mode occurred.

During the research of Bakker, the yield eye mechanism was observed three times for small corner radii and for the highest η ratios. It was believed that this yield eye mechanism occurred due to a not rigidly fixed load bearing plate. Now it can be concluded that this yield eye mechanism is a normal failure mechanism and is not caused by questionable testing conditions.

3.3 APPEARANCE OF THE BENDING MECHANISM FOR A SMALL CONCENTRATED LOAD AND BENDING MOMENT

The bending mechanism for pure bending moment is presented in 1.2. The yield eye mechanism for concentrated load and large bending moments is presented in 2.4.1. It is not known whether for very high η ratios, the yield eye mechanism or the bending mechanism occurs. This will be investigated using numerical simulations in which sections can be tested with very high η ratios. Using these simulations, knowledge can be obtained about the influence of a (small) concentrated load on the behaviour of sections subjected to a large bending moment.

3.4 REDISTRIBUTION OF BENDING MOMENTS

In 1.2 the moment redistribution phenomenon is presented. In 2.3.4. the bending moment-support rotation for the tested sections is presented in 2.4.1. For these sections, it is questionable whether moment redistribution is allowed, because the bending moment decreases sharply after the ultimate bending moment is reached. Rotation capacity is limited.

4 CONCLUSIONS

- A pilot test series was carried out with specimens with small corner radii, giving *M/F* and η ratios as found in practice. The 'bending and rebending' zone had no influence on the type of failure. Further experimental work will be carried out to test the definite test series with sections without the 'bending and rebending' zone.

- For sections having small corner radii and subjected to a concentrated load and a medium to large bending moment, two failure modes occur: a yield arc mode and a yield eye mode.

- After the ultimate load, three yield line mechanisms occur: a yield arc mechanism, a yield eye mechanism, and an interaction mechanism.

- It is questionable whether moment redistribution can be used for sections with small corner radii. For all failure mechanisms rotation capacity is limited.

- The yield eye mechanism found in the tests show that during the research of Bakker, the assumption that this mechanism is caused by a not fully fixed load bearing plate was incorrect.

REFERENCES

[Bakk86a] Bakker, M. and Peköz, T., 1986, Comparison and evaluation of web crippling prediction formulas, EUT-report 86-B-01, Eindhoven University of Technology.

[Bakk92a] Bakker, M., 1992, Web crippling of cold-formed steel sections, Dissertation Eindhoven University of Technology, The Netherlands.

[Dann90a] Dannemann, Robert, W. Effective Width in Elastic Post-Buckling of Thin Flanges, Tenth International Specialty Conference on Cold-formed Steel Structures, St. Louis, Missouri, USA, 1990.

[Euro88a] Eurocode 3, Design of Steel Structures. Part 1: general rules and rules for building. Final Draft. Brussels, CEC

[Hair95a] Haironville Nederland, Leveringsprogramma en fabriekstekeningen profielen, Haironville Nederland, Rotterdam, NL

[Hofm96a] Hofmeyer, H., Kerstens, J.G.M., Snijder, H.H., Bakker, M.C.M. New Research Directions in Flexural Section Failure at an Interior Support (interaction of web crippling and bending moment). European Workshop Thin-Walled Steel Structures, September 26-28, 1996, Krzyzowa, Poland.

[Hofm96c] Hofmeyer, H. Literature and Experimental Research (PT Series), Report BKO-TUE, Eindhoven University of Technology. The Netherlands.

[Land94a] Landolfo, Raffaele and Mazzolani, Federico M. Ultimate Behaviour of Trapezoidal Steel Sheets in Bending, Twelfth International Specialty Conference on Cold-Formed Steel Structures, St. Louis, Missouri, USA, 1994.

[Nest80a] Van Neste, A.J. and Van Pelt, F. Effective Width of Steel Compression Elements. An evaluation of some calculation methods by bending and vibration tests. Report THE-BKO-S-80-01. Eindhoven University of Technology, The Netherlands.

[Rein83a] Reinsch, W., 1983, Das Kantenbeulen zur rechnerischen Ermittlung von Stahltrapezbleck-Tragern, Dissertation 17. Darmstadt: Technische Hochschule Darmstadt,

Germany.

[Rgsp85a] Richtlijnen voor de berekening van Stalen Dakplaten RGSP'85, Staalbouwkundig Genootschap, The Netherlands

[Sab95a] SAB-profiel, Leveringsprogramma profielen, SAB-profiel, IJsselstein, NL

[Tsai86a] Tsai, Y.M./Crisinel, M., 1986, Moment redistribution in continuous profiled sheeting. Thin-walled metal structures in buildings. IABSE proceeding 49, pp. 107-114.

[Vaes95a] Vaessen, M. On the elastic web crippling stiffness of thin-walled cold-formed steel sections, Graduate Thesis TUE-BKO-95-17, Eindhoven University of Technology, The Netherlands.

[Wing81a] Wing, B.A. Web crippling and the interaction of bending and web crippling of unreinforced multi-web cold-formed steel sections. M.A. Sc. Thesis, University of Waterloo, USA, 1981.

NOTATION

b_{bf} Bottom flange width, as shown in figure 9.
$b_{bf;fl}$ Flat bottom flange width, as shown in figure 9.
b_m Section width as shown in figure 9.
b_{tf} Top flange width, as shown in figure 9.
$b_{tf;fl}$ Flat top flange width, as shown in figure 9.
b_w Web width, as shown in figure 9.
$b_{w;fl}$ Flat web width, as shown in figure 9.
E Modulus of elasticity.
F Concentrated load acting on a section.
f_u Steel ultimate strength.
F_u Section ultimate concentrated load resistance.
f_y Steel yield strength.
h_m Section height, as shown in figure 9.
h_w Section height, as shown in figure 9.
L Section span length.
M Bending moment acting on a section.
M_u Section ultimate bending moment resistance.
$r_{i;bf}$ Interior corner radius between web and bottom flange, as shown in figure 9.
$r_{i;tf}$ Interior corner radius between web and top flange, as shown in figure 9.
r_{bf} Corner radius between web and bottom flange, as shown in figure 9.
r_{tf} Corner radius between web and top flange, as shown in figure 9.
t Steel plate thickness.
q Equally distributed load acting on section.

α Factor used for interaction formula for predicting section behaviour at interior support, empirically determined.
β Factor used for interaction formula for predicting section behaviour at interior support, empirically determined.
ε_u Tensile strain at fracture.
η Ratio between M/M_u and F/F_u.
θ_w Angle between web and top flange, as shown in figure 9.
γ Factor used for interaction formula for predicting section behaviour at interior support, empirically determined.